Check for updates

View Article Online
View Journal

Green
Chemistry

Accepted Manuscript

This article can be cited before page numbers have been issued, to do this please use: L. Vaccaro, F. Ferlin, M. Cappelletti, R. Vivani, M. Pica and O. Piermatti, *Green Chem.*, 2019, DOI: 10.1039/C8GC03513J.

Volume 18 | Number 7 | 7 April 2016 | Pages 1821–2242

Green
Chemistry

Cutting-edge research for a greener sustainable future
www.rsc.org/greenchem

ISSN 1463-9262

ROYAL SOCIETY OF CHEMISTRY

CRITICAL REVIEW
G. Chatel et al.
Heterogeneous catalytic oxidation for lignin valorization into valuable chemicals: what results? What limitations? What trends?

175 YEARS

This is an Accepted Manuscript, which has been through the Royal Society of Chemistry peer review process and has been accepted for publication.

Accepted Manuscripts are published online shortly after acceptance, before technical editing, formatting and proof reading. Using this free service, authors can make their results available to the community, in citable form, before we publish the edited article. We will replace this Accepted Manuscript with the edited and formatted Advance Article as soon as it is available.

You can find more information about Accepted Manuscripts in the author guidelines.

Please note that technical editing may introduce minor changes to the text and/or graphics, which may alter content. The journal's standard Terms & Conditions and the ethical guidelines, outlined in our author and reviewer resource centre, still apply. In no event shall the Royal Society of Chemistry be held responsible for any errors or omissions in this Accepted Manuscript or any consequences arising from the use of any information it contains.

ROYAL SOCIETY
OF CHEMISTRY

rsc.li/green-chem

View Article Online
DOI: 10.1039/C8GC03513J

Journal Name

ARTICLE

Au@Zirconium-Phosphonate Nanoparticles as Effective Catalytic System for the Chemoselective and Switchable Reduction of Nitroarenes

Received 00th January 20xx,
Accepted 00th January 20xx

DOI: 10.1039/x0xx00000x

www.rsc.org/

Francesco Ferlin,[a] Matteo Cappelletti,[a] Riccardo Vivani,[b] Monica Pica,*[b] Oriana Piermatti,*[a] and Luigi Vaccaro *[a]

In the present paper, a novel inorgano-organic layered material, a zirconium phosphate aminoethyl phosphonate, ZP(AEP), bearing aminoethyl groups on the layer surface, was used to immobilize AuNPs by a two step procedure. The gold-based catalyst, Au1@ZP(AEP), containing 1 wt% Au, was characterized in terms of physico-chemical properties and TEM analysis revealed that the AuNPs have a spherical shape and an average size of 7.8 (± 2.4) nm. Au1@ZP(AEP) proved its high efficiency for the chemoselective reduction of nitroarenes under mild conditions. Both batch and flow conditions protocols have been defined. The catalytic system has been proven to be able to easily switch chemoselectivity allowing to control the reduction of a series of nitroaromatics towards their corresponding azoxyarenes (**2a-k**) or anilines (**2a-l**) in EtOH 96% or EtOH abs, respectively, by using $NaBH_4$ as reducing agent, in good to excellent yield. Recovery and reuse of the catalytic system has been investigated proving the benefits of the flow approach.

Introduction

Modern and efficient synthetic methodologies rely on the definition and use of efficient catalytic systems able to permit the access to the desired product with high chemical and environmental efficiency.[1]

Although industrial production may still prefers the use of well-established homogeneous methods,[2] heterogeneous catalytic systems feature evident advantages in terms of easier recovery provided that the catalyst does not lose activity during the reuse. Heterogeneous catalytic systems may also offer the additional advantage to control a change in selectivity and possibily increase the catalytic stability/efficiency. They should be appealing from both the chemical and sustainability point of views.[3]

Our research is aimed at the definition of green and sustainable protocols for organic transformations based on the use of safer/sustainable reaction media,[4] and on the preparation and use of recoverable catalytic systems adequate for being used in continous-flow reactors and featuring a minimal leaching.[5] These aspects are of key interest in the context of green chemistry, where chemical efficiency has to be combined with economic and environmental needs.[1-3]

Noble metals are well known and widely studied heterogeneous catalysts in several fields. Due to their expensiveness, they are generally used in low amounts and in the form of nanoparticles, which assure a large fraction of metal atoms exposed on the surface.[6] Moreover, their use in catalyzed sustainable industrial processes needs that they can be easily handled and recovered. In order to prevent the metal nanoparticle (MNP) aggregation and enabling the catalyst recovering and reuse, MNPs can be dispersed on solid supports.[7]

Supported gold NPs (AuNPs) are largely used as catalytic systems for promoting a plethora of transformations, including oxidations, hydrogenations and C–C bond forming processes.[8] Among these, the selective reduction of nitroaromatics into aniline, azo-, and azoxy-compound is an important process because these moieties are often endowed in active natural products, dyes, pigments, agrochemicals and pharmaceuticals.[9] A large number of procedures have been developed for the reductive transformation of nitroarenes.[10] Very few examples exist in the literature where a single reducing system is able to chemoselectively reduce nitroaromatic compounds into only one of the possible reductive products (e.g, aniline, or azo-, or azoxy-compounds) and that it is also capable of switching its selectivity to access a different prouct by varying the reaction conditions.[11]

Immobilized AuNPs have been widely used for the selective reduction of nitroarenes to anilines by using $NaBH_4$,[12] silane,[12a,13] formic acid[14] as reducing agents, while only few examples report the preparation of azo[15] or azoxy compounds[16] by using 2-propanol as reducing agent by light activation. The chemoselective preparation of all three compounds were reported by Liu at al. by using supported AuNPs on *meso*-CeO_2

---

[a] *Laboratory of Green Synthetic Organic Chemistry – Dipartimento di Chimica, Biologia e Biotecnologie, Università di Perugia Via Elce di Sotto, 8 - 06123 Perugia, Italy. E-mail: luigi.vaccaro@unipg.it; Web: www.dcbb.unipg.it/greensoc*
[b] *Dipartimento di Scienze Farmaceutiche, Università di Perugia, Via del Liceo, 1, 06123 Perugia, Italy*

Electronic Supplementary Information (ESI) available: [experimental procedures and calculation, copies of ^1H and ^{13}C NMR spectra. See DOI: 10.1039/x0xx00000x

View Article Online
DOI: 10.1039/C8GC03513J

and 2-propanol/water combination as reducing agent at 30-80 °C to obtain azoxy-, azo-, or aniline compounds with high yield.[11c]

The development of a mild and chemoselective catalytic system which allows to obtain more than one target product by easily controlled switchable reduction conditions is still of great importance.

It is known that the catalytic activity of AuNPs significantly decreases for particle size above 10 nm.[17] In light of this, the key point in the design of supported AuNPs catalysts is the choice of suitable supports, assuring the NPs retention and preventing their aggregation or coalescence. Besides, thiols or amino groups are also known to stabilize AuNPs.[18] In this context, layered zirconium phosphonates and phosphates with high surface area can offer attractive supports for metal nanoparticles[19] because of their chemical and thermal stability together with a facile tunability of their structural features.[19,20]

Layered compounds with an α-type structure consist of planes of zirconium atoms bonded through monohydrogen phosphate groups, O_3POH and/or phosphonate groups, O_3PR.[21]

To our knowledge, no examples are reported in the literaure on AuNPs supported on α-zirconium phosphates or phosphonates. With this aim, we decided to investigate the use of a new taylor-made inorgano-organic material, bearing amino groups covalently bonded to an inorganic backbone, as support for AuNPs. Specifically, in the present paper the synthesis of a new nanosized zirconium phosphate aminoethylphosphonate (ZP(AEP)x) was reported. ZP(AEP)x was prepared by topotactic anion exchange reaction of part of the phosphate groups of nanocrystalline α-zirconium phosphate (α-ZP) with aminoethylphosphonate groups. Then, the particle surface of the support was decorated with AuNPs through a two step procedure, involving the adsorption of Au(III) species on the solid surface, followed by reduction with $NaBH_4$. The Au@ZP(AEP) catalysts, containing 1 and 2.4 wt% AuNPs, were then characterized by Transmission Electron Microscopy (TEM), X-Ray Powder Diffraction (XRPD) and UV–Vis Diffuse Reflectance Spectroscopy (DRS) analysis. Finally, the catalyst with 1 wt% Au loading was used for the selective reduction of nitroarenes, under green and mild conditions, for the preparation of anilines and azoxyarenes both under batch and continuous flow conditions.

Results and Discussion

Catalyst synthesis and characterization. In previous works it has been proven that, differently from microcrystalline α-type ZP, nanocrystalline α-ZP is able to give topotactic anion exchange reactions with phosphonic acids in relatively mild conditions,[22] providing single phase zirconium phosphate-phosphonate compounds, where the phosphate and phosphonate groups are randomly arranged in the structure. The higher reactivity of nanosized ZP, with respect to the corresponding microcrystalline compound, has been ascribed both to the larger amount of surface exposed to the solution, and to the higher fraction of low coordinated edge phosphate groups, which can be replaced by phosphonate groups more easily than the tridentate HPO_4 groups typical of microcrystalline α-ZP.

In the present paper, a gel of nanosized α-ZP in propanol reacted with different amounts of aminoethylphosphonic acid (H_2AEP) to obtain zirconium phosphate aminoethylphosphonates, $ZP(AEP)_x$, with different amounts of aminoethyl groups. Due to the low solubility of H_2AEP in propanol, the reaction was carried out in a 1:1 v/v PrOH:H_2O solution, at 80 °C. The P_{tot}/Zr molar ratio of the $ZP(AEP)_x$ obtained samples, determined by ICP-OES analysis, was 2 in all cases, so that the following general composition can be assigned:

$$Zr(O_3PC_2H_4NH_2)_x(O_3POH)_{2-x}.$$

Then, the x values have been calculated from the phosphonate/phosphate molar ratios (hereafter AEP/P) obtained by ^{31}P liquid NMR; the corresponding NMR spectra were reported in Figure S1, while the calculated x values are shown in Table 1.

Table 1. Composition of the $ZP(AEP)_x$ compounds obtained for different H_2AEP/Zr molar ratios in the starting reacting mixture.

H_2AEP/Zr^a	P_{tot}/Zr^b	AEP/P^c	x
1.0	2.0	0.56	0.72
2.0	2.0	0.64	0.78
3.0	2.0	0.85	0.92
1.0	2.0	0.56	0.72

[a]Molar ratio in solution; [b]Molar ratio in the solid, calculated by ICP analysis; [c]Molar ratio in the solid, Calculated by ^{31}P liquid NMR analysis.

Thermogravimetric analysis profiles of ZP(AEP)x were reported in Figure S2. They show a first weight loss at ca. 100 °C, due to intercalated/adsorbed water and/or solvent, and a second loss in the range 200-800 °C, due to the decomposition of the organic moieties and to the loss of condensation water. From the second weight loss it is generally possible to calculate the formula weight of the compound. It is noteworthy that, despite the uncertainty of the TG data, due to the partial overlapping of dehydration and decomposition steps, the calculated formula weights of the materials are in good agreement with those obtained by ICP-OES and ^{31}P liquid NMR, with a maximum difference of 7%. Figure 1 shows the XRPD patterns of the ZP(AEP)x samples, together with that of the unmodified nanosized ZP, for comparison.

View Article Online
DOI: 10.1039/C8GC03591J

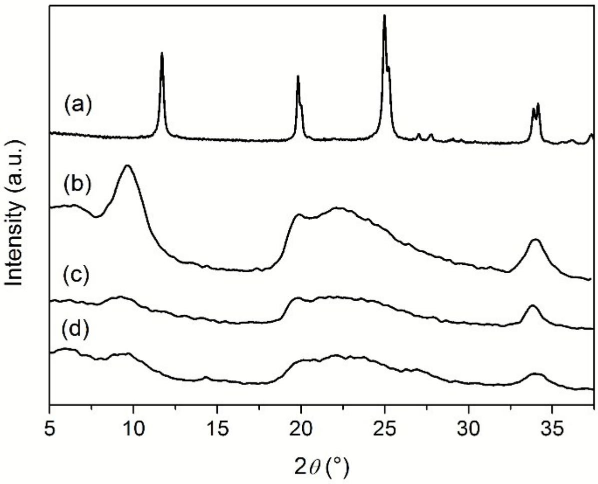

Figure 1. XRPD patterns of: nanosized ZP (a); ZP(AEP)$_{0.72}$ (b), ZP(AEP)$_{0.78}$ (c), ZP(AEP)$_{0.92}$ (d).

Differently from pristine nanosized ZP, the ZP(AEP)$_x$ samples are almost amorphous and few broad peaks are observed in the corresponding XRPD patterns. However, some structural considerations can be attempted: 1) the peak of ZP at 33.8° 2θ, associated with the Zr−Zr separation in the α-type layer (the *(020)* reflection of α-ZP), was still observed in the pattern of ZP(AEP)$_x$. This fact is in agreement with previous works, which proved that the replacement of phosphonate groups for monohydrogen phosphate groups maintained unaltered the structure of the α-type layer to some extent.[22] 2) The patterns of the ZP(AEP)$_x$ samples show a broad peak around 9.8° 2θ, that can be attributed to a phase with an interlayer distance of ≈ 9 Å: this value lies between those of the pure Zr aminoethylphosphonate $Zr(O_3PC_2H_4NH_2)_2$ (d = 11.3 Å)[23] and pure monohydrate α-ZP (d = 7.6 Å). Moreover, the peak associated to the interlayer distance of the parent monohydrate α-ZP at 11.65° was never observed. These results are in agreement with previuos data on the topotactic exchange reactions of nanocrystalline ZP with aryl- and alkylphosphonic acids[22] and suggest that single phase mixed compounds, containing randomly distributed phosphate and aminoethylphosphonate groups on the surface of layers with an α-type structure, are formed. Moreover, the coexistence of free –$C_2H_4NH_2$ and –POH groups between adjacent layers let to suppose that –NH_3^+ PO^- interactions can occur to some extent.

An approximate prediction of the interlayer distance of a mixed phosphate aminoethylphosphonate compound can be obtained by a simple structural model, starting from the α-type crystallographic structure of $Zr(PC_2H_4NH_3Cl)_2$, solved from XRPD data in our laboratory, and by replacing a half of aminoethyl groups with -OH groups. Interlayer chlorine atoms, present in the starting structure,were also eliminated. In this model, the stacking of adjacent layers was set taking into account that the amino groups af a layer can interact via hydrogen bonds with P-OH groups (N···O distance ≈ 2.8 Å) of adjacent layers, and no other close contact is present among groups in the interlayer region, as shown in Figure 2. The interlayer distance, estimated according to the model of Figure 2, is in perfect agreement with the experimental value of 9 Å.

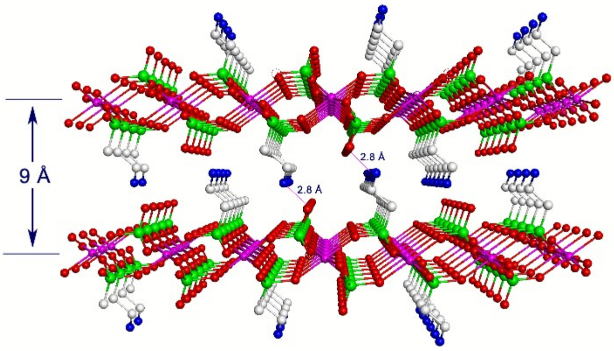

Figure 2. Ideal representation of an α-Zr phosphate in which a half of phosphates have been replaced by aminoethylphosphonate groups.

Synthesis and characterization of Au@ZP(AEP). The catalytic activity of AuNPs strongly depends, among other factors, on the particle size and it has been proved that they are highly active when their size is below 10 nm. The use of AuNPs supported and dispersed on a solid matrix is a quite attractive strategy[6] in order to reduce and stabilize the Au particle size, thus preventing them from agglomeration. In light of this, the optimal catalyst loading in Au supported systems is generally in the range 1-3 wt%. In the present paper ZP(AEP)$_{0.72}$ was used as support for AuNPs: samples with 1.0 and 2.4 wt% of Au loading, were prepared through a two-step procedure as reported in the Experimental Section. First, suitable amounts of a $AuCl_4^-$ solution were added to a suspension of ZP(AEP)$_{0.72}$ in water and the mixture was left under stirring at 30 °C for about one day. At first, the solution had a bright yellow color, due to the presence of soluble Au(III) species; then, a progressive decolorization of the solution was observed, while the solid gradually acquired a pale yellow color. It is reasonable to suppose a chemisorption of the $AuCl_4^-$ ions through an ion exchange reaction involving protonated $O_3PC_2H_4NH_3^+$ groups, reasonably located on the layer surface of ZP(AEP)$_{0.72}$ (due to the repeated washings of the solid with acidic solution), according to the following scheme:

$$(\equiv PC_2H_4NH_3^+)_{(s)} + AuCl_4^-{}_{(aq)} \rightarrow (\equiv PC_2H_4NH_3^+AuCl_4^-)_{(s)}$$

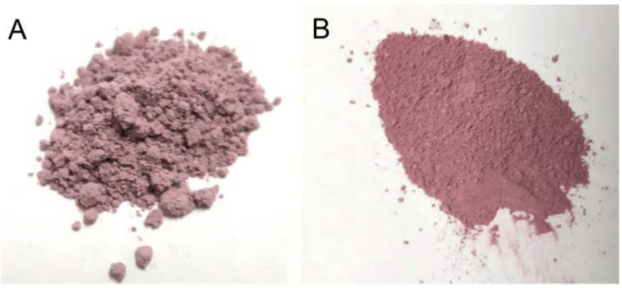

Figure 3. Pictures of Au1@ZP(AEP) (A) and Au2.4@ZP(AEP) (B)

After the addition of the reducting agent, $NaBH_4$, the solution turned to pink/plum, which is the typical color of AuNPs. Gold loadings of 1

View Article Online
DOI: 10.1039/C8GC03513J

and 2.4 wt% were confirmed by ICP analysis. The dried samples are shown in Figure 3 and they will be hereafter labelled as *Au1@ZP(AEP)* (Au loading = 1 wt%) and *Au2.4@ZP(AEP)* (Au loading = 2.4 wt%). Figure 4 shows TEM images of the ZP(AEP)$_{0.72}$ support at two different magnifications, while Figures 5 and 6 show representative TEM images of the Au1@ZP(AEP) and Au2.4@ZP(AEP) samples, respectively, together with the corresponding Au particle size distribution, obtained by analyzing at least 150 nanoparticles.

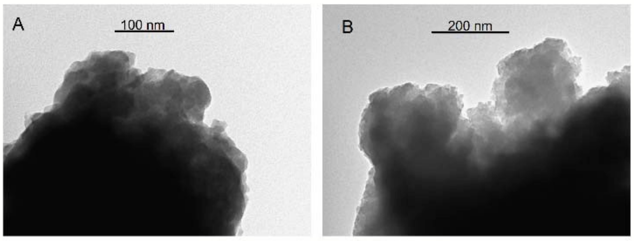

Figure 4. Representative TEM images of ZP(AEP)$_{0.72}$.

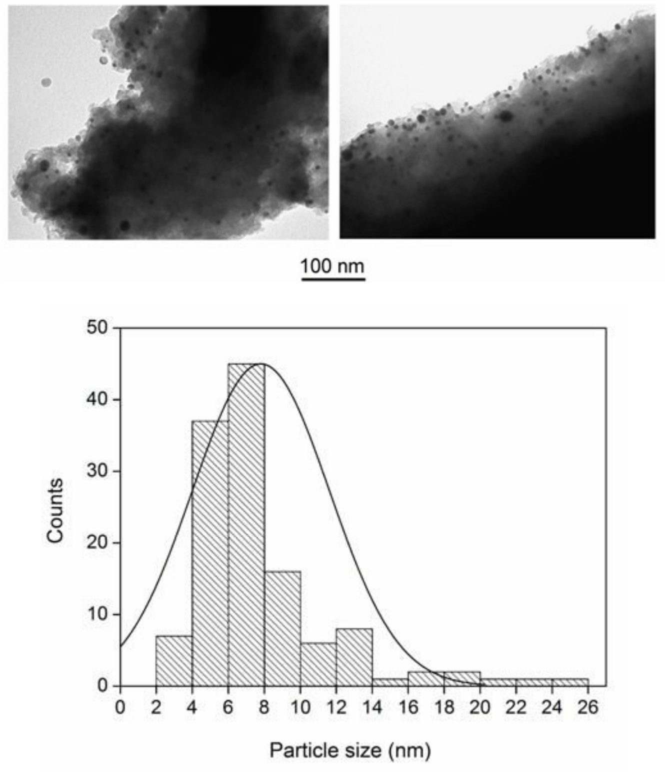

Figure 5. TEM image of Au1@ZP(AEP) and Au particle size distribution.

The support consisted of particle aggregates with irregular size and shape, typical of quite amorphous materials and after treatment with $HAuCl_4/NaBH_4$ the surface of ZP(AEP)$_{0.72}$ aggregates was decorated with AuNPs, exhibiting an almost spherical morphology (Figures 5 and 6). The average particle size increased with increasing the gold loading, being 7.8 (± 2.4) nm and 10.6 (± 5.7) nm for Au1@ZP(AEP) and Au2.4@ZP(AEP), respectively.

Figure 7 shows the XRPD patterns of ZP(AEP)$_{0.72}$, Au1@ZP(AEP) and Au2.4@ZP(AEP). The pattern of ZP(AEP)$_{0.72}$ did not undergo significant changes after treatment with $AuCl_4^-/NaBH_4$. Moreover, the reflection at 38.3° 2θ, corresponding to the *(111)* crystallographic planes of the face-centered cubic Au structure (JCPDS No. 4-784), was observed only at the highest Au loading (pattern (b)).

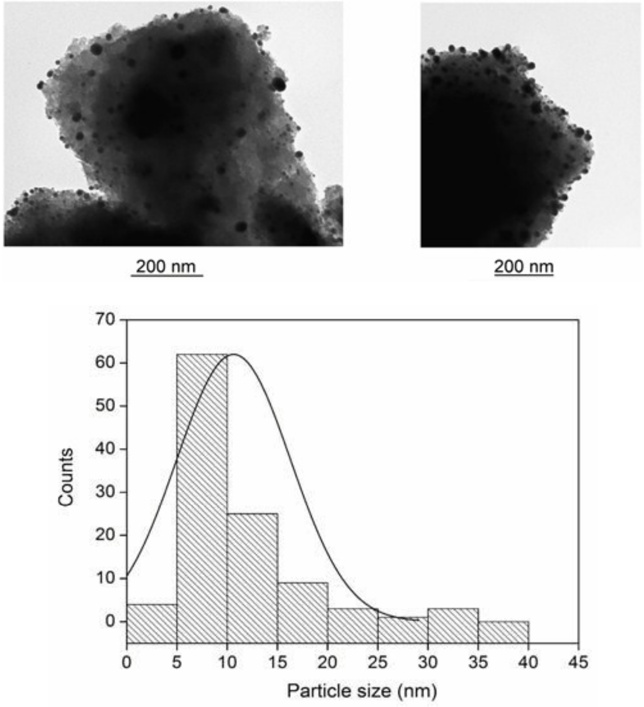

Figure 6. TEM image of Au2.4@ZP(AEP) and Au particle size distribution.

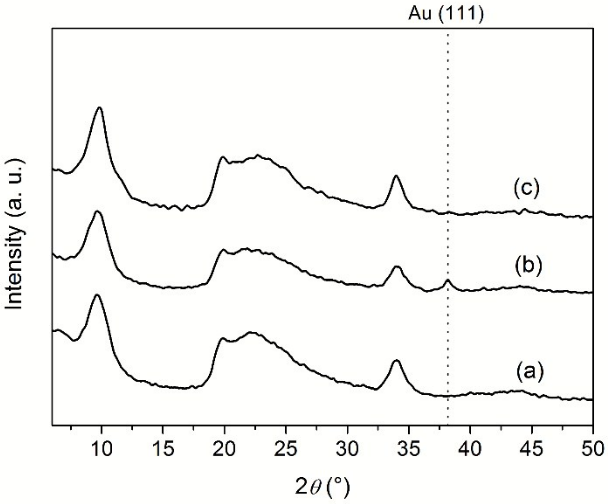

Figure 7. XRPD patterns of ZP(AEP)$_{0.72}$ (a); Au2.4@ZP(AEP) (b); Au1@ZP(AEP) (c).

View Article Online
DOI: 10.1039/C8GC03513J

Figure 8 shows the absorption spectra, in Kubelka–Munk units,[24] of Au1@ZP(AEP) and Au2.4@ZP(AEP): K and S are the absorption and scattering coefficients, respectively. An absorption band in the visible region is observed, due to the surface plasmon resonance of the AuNPs. The presence of just one absorption band indicates that the AuNPs are nearly spherical particles,[25] in agreement with TEM analysis, while the red shift of the absorption maximum (from 527 nm to 530 nm for Au1@ZP(AEP) and Au2.4@ZP(AEP), respectively) is in agreement with the increase of the Au particle size with increasing the Au loading.[26]

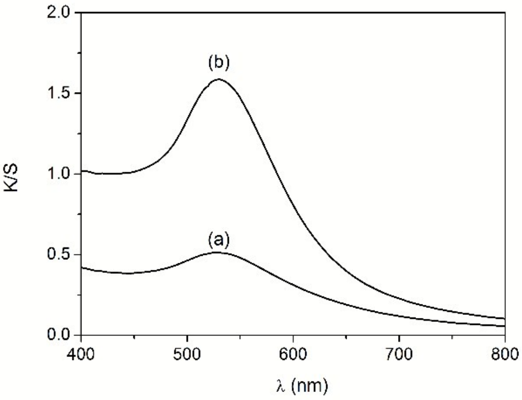

Figure 8. Absorption spectra in terms of the Kubelka–Munk function (K/S) of Au1@ZP(AEP) (a) and Au2.4@ZP(AEP) (b).

FTIR spectrum of ZP(AEP) is shown in Figure 9a. According to the literature, three main absorption regions can be identified.[27] The strong band in the 850-1100 cm^{-1} probably is the result of the crowding of many absorption effects in that region: P-C, P-O, C-N stretching motions, and also the out-of-plane N-H bending absorption. Between 1280 and 1800 cm^{-1} the absorptions of C-NH$_2$, C-NH$_3^+$ and CH$_2$ can be observed. Specifically, the absorptions at 1519 and 1283 cm^{-1} can be assigned to the NH$_3^+$ deformation bands, the band at 1620 cm^{-1} is characteristic of the N-H bending, while the absorption at 1470 cm^{-1} can be assigned to the CH$_2$ bending. Above 2500 cm^{-1} a quite wide band is present and it derives from the stretching of hydrogen bonded NH$_2$, NH$_3^+$, and that from the OH between water and phosphate groups.

The FTIR spectrum of Au1@ZP(AEP) (Figure 9b) is quite similar to that of ZP(AEP), with a general increase of the absorption intensities. This change can be attributed to a variation of the vibrational structure, due to some dipole interactions of the external goups with gold nanoparticles.[28]

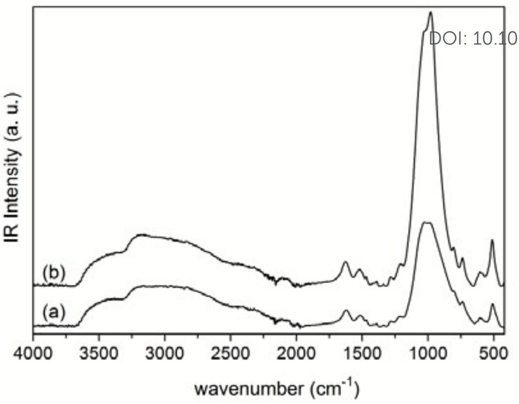

Figure 9. FTIR spectra of (a) ZP(AEP) and (b) Au1@ZP(AEP) samples.

Representative SEM pictures of ZP(AEP) and Au1@ZP(AEP), collected at different magnifications, with both secondary and backscattered electrons, are shown in Figure 10. A quite different morphology was observed for ZP(AEP) and Au1@ZP(AEP). Specifically, while the particle surface of the unloaded support appears smooth (Figure 10A, C), that of Au1@ZP(AEP) exhibits a certain roughness (Figure 10D). Moreover, backscattered electron images of Au1@ZP(AEP) show the presence of bright spots (Figure 10E, F), not observed in ZP(AEP) (Figure 10B), due to AuNPs.

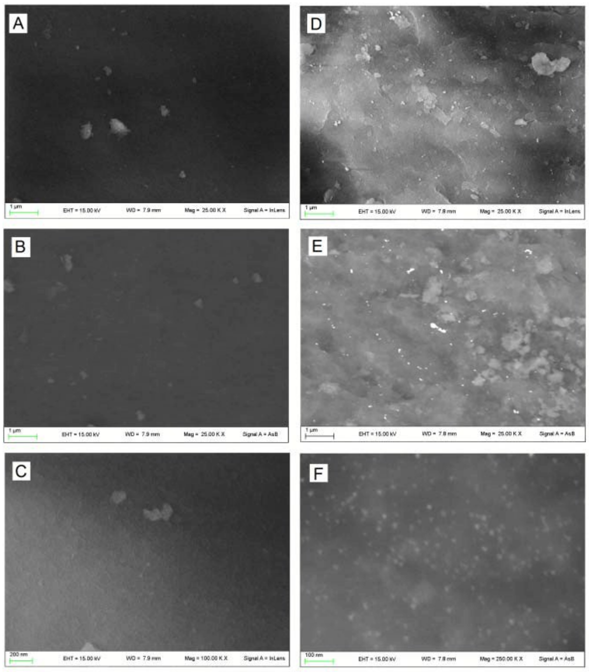

Figure 10. SEM pictures of ZP(AEP) (A, B, C) and Au1@ZP(AEP) (D, E, F) collected by secondary (A, C, D) and backscattered (B, E, F) electrons.

Energy dispersive X-ray (EDX) analysis performed on both samples provided interesting information about the elemental composition of their surface. As shown in Figure 11, besides P, Zr, C, N and O, also Cl was detected in ZP(AEP), confirming the presence of –NH$_3$Cl groups on the surface of the starting material. After treatment with

View Article Online
DOI: 10.1039/C8GC03617J

$HAuCl_4$ and $NaBH_4$, the chlorine peak disappeared, while that of Au appeared, proving the $Cl^-/AuCl_4^-$ anion exchange occurred on the support surface.

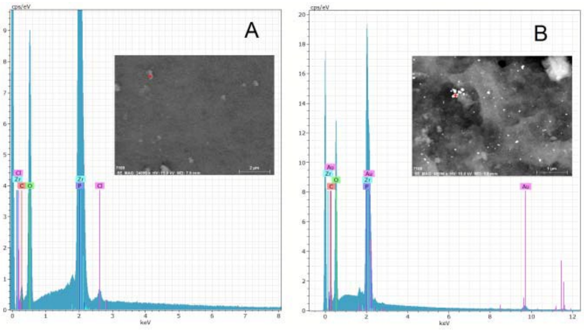

Figure 11. EDX spectra of (A) ZP(AEP) and (B) Au1@ZP(AEP), referred to the areas indicated by the red cross in the corresponding SEM pictures.

Specific surface area, calculated by the BET method, of ZP(AEP) is less than 5 m^2/g, probably due to the tendency of the particles to aggregate during the drying process. After immobilization of gold nanoparticles the surface area increases up to 11 m^2/g, in agreement with that observed in the SEM pictures of Au1@ZP(AEP), showing a more pronounced roughness of the surface, with respect to ZP(AEP). It is reasonable to attribute these modifications to the procedures used for the synthesis of the AuNPs.

Catalytic Activity. Due to its smaller Au particle size, Au1@ZP(AEP) was selected for being used in the catalytic tests on our targeted process, the chemoselective reduction of nitroaromatics. We started our study testing the catalytic activity of Au1@ZP(AEP) in the reduction of 4-nitroanisole (**1a**) in EtOH 96% or EtOH absolute as a representative safe and effective medium for such a process. We have used $NaBH_4$ as reducing agent and after a reaction time of 3 h at 30 °C, we evaluated the different conditions to access the selective preparation of the corresponding azoxy derivative **2a** and the 4-metoxyaniline (**4a**). The reactions were performed in a closed vial paying attention to select the size and the scale of the reactants in order to fill-up the reactor volume with reaction medium (ca. 0.05M). When the reaction was performed in EtOH 96% in presence of 0.5 mol% of Au1@ZP(AEP) and 3 eq of $NaBH_4$ the azoxy derivative **2a** was obtained with high selectivity, but the conversion was low (42%, Table 2, Entry 1). Increasing the reaction temperature to 50 °C, the conversion slightly increases but a lower selectivity was observed (C 47%, **2a**:**3a**:**4a** = 81:18:1, Table 2, Entry 1, note *c*). Increasing the amount of $NaBH_4$ to 6 eq the reactivity and selectivity was unchanged (Table 2, Entry 2). In the presence of 1 mol% of Au1@ZP(AEP) and 3 eq of $NaBH_4$ a conversion 83% was obtained still with a high selectivity of product **2a** (Table 2, Entry 4). A complete conversion with a good selectivity (96%) was obtained in presence of 6 eq. of $NaBH_4$ (Table 2, Entry 4). When the reaction was performed in presence of 1 mol% of Au2.4@ZP(AEP) the conversion was only 42% (Table 2, Entry 4, note *d*).

We also observed that when absolute EtOH ($EtOH_{abs}$) was used as reaction medium, the catalyst was more efficient and in the presence of just 0.5 mol% of Au1@ZP(AEP) a complete conversion can be obtained after 3 h when using 6 eq of $NaBH_4$ (Table 2, Entries 5 and 6 vs. Entries 1 and 2) with a preferential formation of aniline **4a**. Using Au1@ZP(AEP) in 1 mol% in $EtOH_{abs}$ and in the presence of 6 eq of $NaBH_4$, complete conversion and selectivity towards 4-metoxyaniline (**4a**) was obtained after 2 h (Table 2, Entry 8).

Table 2. Optimization of the reaction conditions in the reduction of 1a.

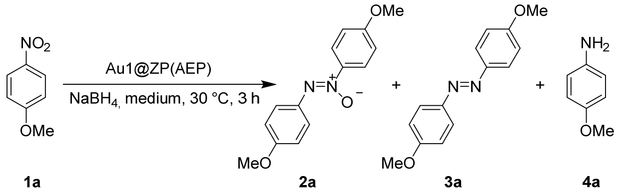

entry[a]	Au1@ZP(AEP) (mol%)	$NaBH_4$ (eq)	Medium	C (%)[b]	2a:3a:4a ratio[b]
1	0.5	3	EtOH 96%	42	98:2:0[c]
2	0.5	6	EtOH 96%	40	97:3:0
3	1	3	EtOH 96%	83	97:3:0[d]
4	1	6	EtOH 96%	99	96:4:0
5	0.5	3	$EtOH_{abs}$	98	87:6:7
6	0.5	6	$EtOH_{abs}$.	99	14:0:86[e]
7	1	3	$EtOH_{abs}$	99	42:1:57
8	1	6	$EtOH_{abs}$.	>99	0:0:100[f]

[a]Reaction conditions: **1a** (0.1 mmol), Au1@ZP(AEP) (0.5 or 1 mol%), $NaBH_4$ (3 or 6 eq), medium (1.8 mL), at 30 °C for 3h. [b] Conversion and product ratios determined by GLC and ^1H-NMR analyses. [c] Reaction temperature 50 °C: C = 47%, 2a:3a:4a = 81:18:1 . [d]Catalyst: Au2.4@ZP(AEP) (1 mol%): C = 42%, 2a:3a:4a = 97:3:0. [e]Reaction time 4 h: C: >99%, **2a**:**3a**:**4a** = 0:1:99. [f] Reaction time 2 h.

Table 3. Substrate scope for the preparation of azoxyderivatives 2a-k.

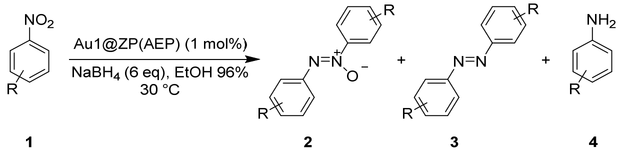

entry[a]	R	t (h)	C (%)[b]	2:3:4 ratio[b]	Y of 2 (%)[c]
1	**a**: 4-OMe	3	99	96:4:0	90
2	**b**: H	2	99	95:5:0	90
3	**c**: 4-Cl	1	99	89:11:0	86
4	**d**: 4-Br	1	>99	85:8:0:7[d]	83
5	**e**: 4-I	1	93	50:7:0:43[e]	44
6	**f**: 4-Me	3	93	98:2:0	88
7	**g**: 3-Me	3	90	90:10:0	78
8	**h**: 2-Me	6	99	95:5:0	92
9	**i**: 3-CH_2=CH_2	3	89	87:13:0	74

View Article Online
DOI: 10.1039/C8GC03513J

10	**j**: 3-COMe	2	95	88:12:0[f]	80
11	**k**: 4-CO2Me	2	99	82:6:0:12[f]	76

[a]Reaction condition: **1** (0.1 mmol), Au1@ZP(AEP) (1 mol%), NaBH$_4$ (6 eq), reaction medium: EtOH 96% (1.8 mL), at 30 °C. [b] Conversion and product ratios determined by GLC and ^{1}H-NMR analyses. [c]Yield of the isolated products **2** after column chromatography. [d] 7% of de-halogenated product was observed. [e] 43% of de-halogenated product was observed. [f] The corresponding hydroxy aryl compound was observed. [g] 12% of *trans*-esterification ethyl ester product was observed.

The preliminary results obtained do not only show the high efficiency of our solid Au-catalytic system, but they also prove that with this catalyst a route towards the chemoselective switchable preparation of **2a** or **4a** is also paved. To evaluate the applicability of these preliminary results, the reaction conditions were extended obtained to a series of nitroarenes **1a-l** with the aim of preparing azoxyderivatives **2a-k** and anilines **4a-l**. Azoxyderivatives **2a-k** have been prepared with very good yields and selectivities performing the reaction in EtOH 96%, by suing 1 mol% of Au1@ZP(AEP) and in the presence of 6 eq of NaBH$_4$ (Table 3). For 4-bromo (**1d**) and 4-iodonitrobenzene (**1e**) an additonal 7% and 43% of de-halogenated products were observed, respectively (Table 3, Entries 4 and 5). In the case of 3-nitroacetophenone (**1j**), the corresponding hydroxyl aryl compound deriving from the reduction of the carbonyl group was isolated (Table 3, Entry 10), while for methyl 4-nitrobenzoate (**1k**) a 12% of trans-esterification product, the ethyl ester derivatives, was isolated (Table 3, Entry 11). The substrate scope for the alternative chemoselective protocol for the preparation of anilines **4** was also investigated. By using EtOH$_{abs}$ as reaction medium, 1 mol% of Au1@ZP(AEP) in the presence of 6 eq of NaBH$_4$, a series of anilines **4** could be prepared with high yields and selectivities. The results are reported in Table 4. For 4-iodonitrobenzene (**1e**) a 75% of de-halogenated product was observed (Table 4, Entry 5) while 4-bromo (**1d**) did not undergo the de-halogenation. The reduction of 3-nitroacetophenone (**1j**) gave rise to the corresponding hydroxy aniline **4j** (Table 4, Entry 10), while methyl 4-nitrobenzoate (**1k**) did not lead to the *trans*-esterification product (Table 4, Entry 11).

Table 4. Substrate scope for the preparation of anilines 4a-l.

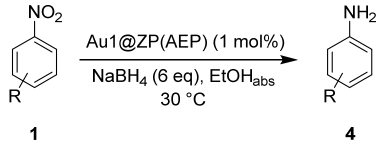

entry[a]	R	t (h)	C (%)[b]	Yield (%)[c]
1	**a**: 4-OMe	2	>99	96
2	**b**: H	2	>99	92
3	**c**: 4-Cl	2	>99	94
4	**d**: 4-Br	2	>99	95
5	**e**: 4-I	1	>99	-[d]
6	**f**: 4-Me	3	>99	98
7	**g**: 3-Me	3	>99	98
8	**h**: 2-Me	6	>99	96
9	**i**: 3-CH$_2$=CH$_2$	6	>99	97
10	**j**: 3-COMe	5	>99	98
11	**k**: 4-CO$_2$Me	4	>99	96
12	**l**: 6-nitroquinoline	4	>99	94

[a]Reaction condition: **1** (0.1 mmol), Au1@ZP(AEP) (1 mol%), NaBH$_4$ (6 eq), reaction medium: EtOH$_{abs}$ (1.8 mL), at 30 °C. [b] Conversion and product ratios determined by GLC and ^{1}H-NMR analyses. [c]Yield of the isolated products **4**. [d] 75% of de-halogenated product was observed.

The recovery and the reuse of the solid catalyst has been performed both in EtOH 96% and EtOH$_{abs}$ in the representative reduction of 4-nitroanisole (**1a**) (Table 5). For each reuse the catalyst was separated by centrifugation, washed with EtOH, aqueous HCl 10^{-2} M to eliminate the borate, water and eventually with EtOH, dried at 130 °C for 15 h and reused in the next run. The solid catalyst was used five consecutive times without loss of activity and selectivity in EtOH$_{abs}$, and only a small reduction in the catalytic activity was observed in EtOH 96% but most importantly the chemoselectivity did not change (Table 5). The ICP-OES analysis of crude products obtained during the five consecutive run by usual work-up procedure (filtration, distillation of EtOH, extraction with ethyl acetate/H$_2$O to eliminate the inorganic reagents, distillation of solvent under reduced pressure), showed a very low content of gold (2.7 ppm). As confirmation of this data, the Au content on the recovered catalyst was determined by ICP-OES analysis showing that the content of gold remained almost unchanged (0.96-1.05 wt% *vs.* 1.0 wt % of pristine catalyst). These results are of additional support to show that the aminoethyl- and the phosphate groups on the surface of support are very effective to stabilize the gold nanoparticles.

Table 5. Recovery and reuse of catalyst in the preparation 4-metoxyaniline (4a) and azoxy derivative (2a).

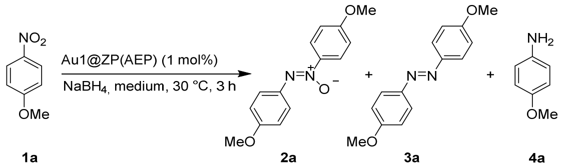

entry[a]	Run	Medium	t (h)	C (%)[b]	2:3:4 ratio[b]
1	Run 1	EtOH 96%	3	98	96:4:0
2	Run 2	EtOH 96%	3	96	97:3:0
3	Run 3	EtOH 96%	3	94	97:3:0
4	Run 4	EtOH 96%	3	93	96:4:0
5	Run 5	EtOH 96%	3	87	98:2:0
6	Run 1	EtOH$_{abs}$	2	>99	0:0:100
7	Run 2	EtOH$_{abs}$	4	>99	0:0:100
8	Run 3	EtOH$_{abs}$	6	>99	0:0:100
9	Run 4	EtOH$_{abs}$	15	>99	0:0:100
10	Run 5	EtOH$_{abs}$	15	>99	0:0:100

[a]Reaction condition: **1** (0.1 mmol), Au1@ZP(AEP) (1 mol%), NaBH$_4$ (6 eq), reaction medium: EtOH 96% (1.8 mL), at 30 °C. [b] Conversion and product ratios determined by GLC and ^{1}H-NMR analyses.

It is well known that the catalytic activity of gold nanoparticles is strongly dependent on the particle size range.[8b] The slight reduction of catalytic activity after recovery and reuse can be explained by comparing the TEM images of the catalyst recovered after five runs in EtOH 96 % or $EtOH_{abs}$ (Table 5). As shown in Figure S3, the AuNPs still have a spherical morphology with good monodispersity and a slight increase of the avearge particle size ranging from 7.8 (± 2.4) nm to 11.4 (± 5.7) and 10.7 (± 6.2) nm, respectively.

For a better evaluation of reusability of Au catalyst the recycle test has been also performed with moderate conversion in $EtOH_{abs}$ at 30 °C for a reaction time of 40 min (see Supporting information, Table 1S). The conversion remained almost constant for five run, only a small reduction in the percentage of the expected 4-methoxy aniline (**4a**) was observed showing a moderate reduction of catalytic activity, likely determined by the moderate increase of Au particles size.

The two reaction pathways can be effectively switched by simply tuning the solvent properties. We also decided to investigate the use of Au1@ZP(AEP) catalyst under continuous flow conditions with the aim of evaluating itsdurability and of definining a simple and greener protocol to achieve the two possible products **2** or **4**. Catalyst Au1@ZP(AEP) was mixed with glass beeds (1mm of diameter), and charged into a stainless steel column and the system was sealed with appropriate screw caps and with connection tubes. After an initial and necessary additional optimization of the flow conditions, we found that benefits arise using the flow approach. In fact, the amount of $NaBH_4$ could be reduced to 3 eq (Table 6, Entry 6) without any loss in efficiency of the reaction. Further optimization regarding the identification of the appropriate residence time to achieve complete conversions, in continuous flow conditions the reduction process could be completed in only 50 min.

Table 6. Optimization of the flow in the preparation of 4-metoxyaniline 4a and azoxy derivatives 2a with Au1@ZP(AEP) as catalyst.

entry[a]	$NaBH_4$ (eq)	Flow rate (mL·min-1)	C to 4a (%)[a]	C to 2a (%)[b]	2a:3a Ratio[c]
1	6	0.5	87	85	84:16
2	6	0.25	95	92	90:10
3	6	0.1	>99	>99	92:8
4	3	0.5	73	70	87:13
5	3	0.25	92	90	90:10
6	3	0.1	>99	>99	93:7
7	2	0.25	84	80	89:11
8	2	0.1	95	95	90:10

[a]Reaction condition: **1a**, Au1@ZP(AEP) (0.2 mol%), $NaBH_4$ (3-6 eq), $EtOH_{abs}$ (0.25M), at 30 °C. [b] **1a**, Au1@ZP(AEP) (0.2 mol%), $NaBH_4$ (3-6 eq), EtOH 96% (0.25M), at 30 °C. [c]Conversion and product ratios determined by GLC and ^{1}H-NMR analyses.

View Article Online
DOI: 10.1039/C8GC03513J

With the optimal conditions we were able to set-up an efficient continuous flow production of azoxy derivative **2a** and aniline **4a** starting from simple 4-nitroanisole (**1a**). For both protocols we observed a strong increase in TON and TOF value (Table 7). These features were all related to the fact that switching from batch to flow condition there is an increase in efficiency and stability of the catalyst that derived from his stable packing inside the reactor.

This evaluation was also supported by the fact that a careful measure of the gold species released (leached) in solution reveals that just a minimal part of the gold catalyst was lost during the reaction. Indeed, the ICP-OES analysis showed that the leaching of gold in solution is constant during the time of the experiments in flow and is below 0.1 ppm (Fig. 12).

Table 7. Comparison of TON and TOF values from batch to flow in the preparation of 4-metoxyaniline (4a) and azoxy derivatives 2a with Au1@ZP(AEP) as catalyst.

	TON	TOF (h^{-1})
BATCH	**4a:** 500 **2a:** 468	**4a:** 50 **2a:** 31
FLOW	**4a:** 5000 **2a:** 7500	**4a:** 600 **2a:** 600

[a]Reaction condition: **1a**, Au1@ZP(AEP) (0.2 mol%), $NaBH_4$ (3-6 eq), $EtOH_{abs}$ (0.25M), at 30 °C. [b] **1a**, Au1@ZP(AEP) (0.2 mol%), $NaBH_4$ (3-6 eq), EtOH 96% (0.25M), at 30 °C. [c]Conversion and product ratios determined by GLC and ^{1}H-NMR analyses.

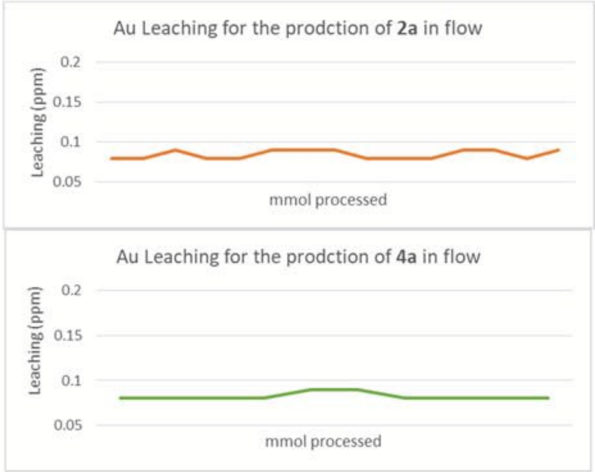

Figure 12. Leaching for the flow procedure in the preparation of 4-metoxyaniline (**4a**) and azoxy derivatives **2a** with Au1@ZP(AEP) as catalyst, in EtOH 96 % (red line), and $EtOH_{abs}$ (green line).

Exploiting the continuous flow reactors, we were indeed able to selectively convert 4-nitroanisole (**1a**) to the corresponding aniline in almost quantitative yields. Equally good results were obtained for the production of azoxy derivatives **2a** where the selectivity was constantly excellent (Figure 13). Considering that the flow reactor

View Article Online
DOI: 10.1039/C8GC03543J

allows to avoid all of the usual steps consisting in the filtration and washing of the catalyst, we have also achieved a significant a decrease in the waste produced resulting in low E-factor values associated to the process (See experimental section).

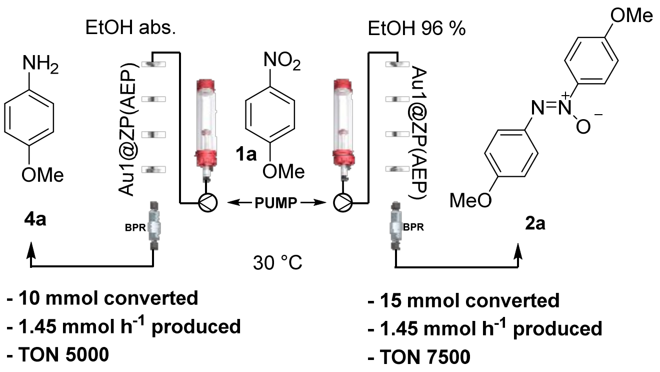

Figure 13. Features of the flow procedure in the preparation of 4-metoxyaniline (**4a**) and azoxy derivatives **2a** with Au1@ZP(AEP) as catalyst.

The ICP-OES analysis performed on solid catalyst recovered after flow procedure for the production of 4-metoxyaniline **4a** and azoxy derivatives **2a** show a Au content of 1.03 wt% and 0.94 wt%, respectively, very still to pristine catalyst value (1.0 wt%). TEM images of catalyst recovered after flow procedure in EtOH 96 % and EtOH abs. (Figure 14) show that the AuNPs still have a nearly spherical morphology with good monodispersity but also that the particle size range are kept small, very close to the starting material (7.9 (± 2.7) and 9.4 (± 3.9) nm, respectively *vs* 7.8 (± 2.4) nm for the pristine material). The flow procedure improves the performance of the catalyst with respect to the batch procedure since the absence of mechanical stirring preserves the characteristics of the catalyst, improving recovery and reuse.

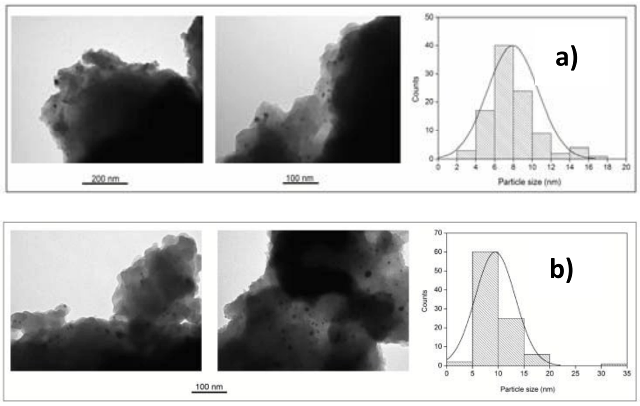

Figure 11. Representative TEM image of Au1@ZP(AEP) after 15 runs in EtOH 96 % (a) and after 10 runs in EtOH$_{abs}$ (b) under fow conditions

Mechanistic Pathway. We observed that, both in EtOH 96% and EtOH$_{abs}$, the mixture during the reaction performed in a closed vial was uncolored but when the vials was opened, under air, the reaction mixture obtained in EtOH 96% quickly turned to yellow while that obtained in EtOH$_{abs}$ remained colorless. Recent papers suggest that in-situ formed gold hydride [Au-H] is responsible for the reduction of nitroarenes.[12a,12e] To rationalize a possible mechanistic pathway that explained the observed selectivity for the reduction in EtOH 96% and EtOH$_{abs}$, we perform the reduction process in CD_3OD. In this experiment, 0.1 mmol of 4-nitroanisole (**1a**), 0.5 mol% of Au1@ZP(AEP), 0.3 mmol of $NaBH_4$ in 1.8 mL of CD_3OD were stirred in a closed vials for 20 min. The evolution of reaction was monitored by NMR spectroscopy directly after quickly filtration on celite. The NMR spectrum performed immediately after filtration showed a conversion >99%, the 4-metoxyaniline (**4a**) and the corresponding hydroxylamine **5a** (**4a:5a** = 55:45) were present together with small a amount of the corresponding azoxy-derivative **2a**. No significant amount of nitroso-, azo- or hydrazo-derivatives were detected (Figure S4a). After 1 h the mixture turned yellow and the NMR spectrum showed the disappearance of hydroxylamine **5a** with the formation of the azoxy-derivative **2a** (**4a:2a** = 56:44) (Figure S4b). Performing the reaction in CD_3OD/D_2O (96:4) the conversion was 94% and the NMR spectrum performed immediately after filtration, showed the 4-metoxyaniline (**4a**), the hydroxylamine **5a** and the azoxy-derivatives **2a** (9:76:15) (Figure S5a) with additional traces of azo-derivative **3a**. After 1 h, almost all the hydroxylamine **5a** was converted in azoxy-derivative **2a** (**4a:2a** = 10:90) (Figure S5b). According to these results, the presence of water plays a crucial role on the catalytic activity of gold nanoparticles and consequently on the mechanistic pathways. Therefore, when the reduction of nitroarenes is performed in EtOH$_{abs}$ the catalytic activity of gold nanoparticles is higher, there was no accumulation of intermediate **5a** that quickly undergoes the successive reduction to 4-metoxyaniline **4a** (Scheme 1, pathway **a**).[12a,12e] When the reduction of nitroarenes is performed in EtOH 96%, the presence of water inhibits the catalytic activity of gold nanoparticles, there is accumulation of the hydroxylamine **5a** that in the presence of air turns to azoxy-derivative **2a** (Scheme 1, pathway **b**).

View Article Online
DOI: 10.1039/C8GC03513J

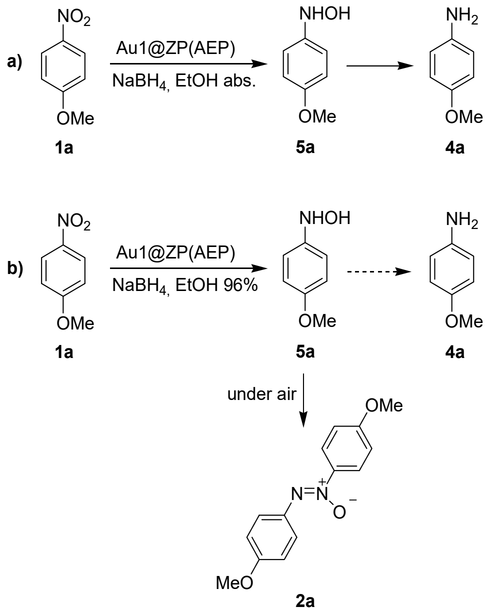

Scheme 1. A plausible reaction pathways for reduction of nitrobenzene in $EtOH_{abs}$ (a) and EtOH 96% (b).

Conclusion

In conclusion, we have reported the novel and efficient preparation of AuNPs immobilized on a novel inorgano-organic layered material, a zirconium phosphate aminoethyl phosphonate, ZP(AEP), bearing aminoethyl groups on the layer surface. The gold-based catalyst, Au1@ZP(AEP), containing 1 wt% Au, was fully characterized. Au1@ZP(AEP) proved to be highly efficient for the chemoselective reduction of nitroarenes under mild conditions. Both batch and flow condition protocols have been defined proving the benefits of the flow approach both in terms of chemical and environmental efficiency. We have been able to control the reduction of a series of nitroaromatics and switch the chemoselectivity towards azoxyarenes (**2a-k**) or anilines (**4a-l**) using EtOH 96% or $EtOH_{abs}$, respectively. Recovery and reuse of the catalytic system has been investigated proving the benefits of the flow approach.

Experimental section

General

Aminoethylphosphonic acid ($H_2O_3PC_2H_4NH_2$, hereafter H_2AEP) was purchased from Epsilon Chimie, France. Hydrogen tetrachloroaurate (III) were purchased from Alfa Aesar. Zirconyl propionate ($ZrO_{1.27}(C_2H_5COO)_{1.46}$, MW = 218 Da) was supplied by MEL Chemicals, England. All other reagents were supplied by Aldrich and were used as received without further purification.

XRPD patterns were collected with a Philips X'Pert PRO MPD diffractometer operating at 40kV and 40mA, with a step size 0.03341 and step scan 40 s, using CuKα radiation and an X'Celerator detector. To minimize preferred orientations, the powder samples were carefully side-loaded onto a glass sample holder.

Thermogravimetric analysis was carried out by a NETZSCH STA449 Jupiter thermal analyzer connected to a NETZSCH TASC 414/3 A controller at a heating rate of 10 °C/min, with an air flow of about 30 mL/min.

Quantitative solution phase ^{31}P NMR spectra were measured on a Bruker Advance III HD 400 spectrometer equipped with a smartprobe using the standard inverse-gated decoupling pulse sequence available on the Bruker TopSpin 3.2 library. The relaxation delay was set to 30 s and 16 to 32 scans were collected for each spectrum. Referencing is relative to external 85% D_3PO_4 in D_2O. Each NMR sample was prepared by dissolving about 10-15 mg of the solid in 3 M HF (≈0.1 mL) and adding about 0.5 mL of D_2O.

^1H-NMR, ^{13}C-NMR spectra were recorded at 400 MHz and 100.6 MHz, respectively, on a Bruker DRX-ADVANCE 400 MHz.

Zr, P and Au analyses were performed on an ICP Varian Liberty inductively-coupled plasma-optical emission spectrometry (ICP-OES) with axial injection. Gold-free solid samples were dissolved with 3 M HF, while the gold-based solid samples were dissolved by treatment with 3 M HF, followed by treatment with a suitable volume of aqua regia.

Transmission electron microscopy (TEM) analysis was carried out by a Philips 208 transmission electron microscope, operating at an accelerating voltage of 100 kV. Powders were rapidly diluted in water, then supported on copper grids (200 mesh) precoated with Formvar carbon films and quickly dried.

Diffusive reflectance measurements were carried out by using a portable spectrophotometer consisting of Avantes parts and a deuterium-halogen lamp (AvaLight-DH-2000-FHS). The reflectance signals were colllceted by an integrating sphere with a 6 mm diameter viewing aperture and 88 irradiation angle (ISP-30-6) and transferred to an AvaSpec–2048 charge-coupled device (CCD) detector via a quartz fiber-optic system (diameter 600 μm). The acquisition of the spectra in the range 200 – 1100 nm was controlled by the AvaSoft software. The experimental values of the reflectance, R, were normalized and used to calculate the K (absorption)/S (scattering) coeffficient ratios according to the following algorithm: $K/S = (1-R)^2/2R$, in agreement with the Kubelka-Munk theory.[24]

Infrared measurements were performed in the 300-5000 cm-1 range at 2 cm^{-1} resolution by ALPHA-FTIR spectrometer of Bruker-Optics, and ATR sampling on a diamond crystal by Platinum-ATR module.

SEM analysis was performed by a Zeiss LEO 1525 FE SEM, equipped with a Angle selective Backscattered detector (AsB) for high energy backscattered electrons imaging, at the LUNA Laboratory of the Department of Physics and Geology of Perugia University. The powder samples were put on an aluminum stub precoated with a double sided adhesive conductive carbon tape.

Nitrogen adsorption/desorption isotherms at 77 K were measured using a computer-controlled Micrometrics ASAP 2010 adsorption analyzer. The preparation of samples was made by degassing the materials at room temperature, overnight. The specific surface area was calculated by the Brunauer, Emmett and Teller (BET) theory.

GLC analyses were performed by using the Hewlett-Packard HP 5890A equipped with a capillary column DB-35MS (30 m, 0.53 mm), an FID detector and hydrogen as the gas carrier. Gas

View Article Online
DOI: 10.1039/C8GC03513J

Chromatography with Electron Impact Mass Spectrometry (GC-EIMS) analyses were carried out by using a Hewlett-Packard HP 6890N Network GC system/5975 Mass Selective Detector equipped with an electron impact ionizer at 70 eV. Thin layer chromatography analyses were performed with silica gel on aluminum plates (silica gel 60 F254, Fluka). Column chromatography purification was performed with silica gel (230–400 mesh) eluting with hexane/ethyl acetate (98:2–70:30). Melting points were measured on a Büchi 510.

Anilines **4a**–**l** [11c, 12b, 14a, 29, 30] and azoxy-derivatives **2a**–**k** [11, 31, 32] are known compounds, azoxy-derivative **2j** is a new compound.

Preparation of layered zirconium phosphate-aminoethyl phosphonates (ZP(AEP)$_x$)

A gel in propanol (PrOH) of nanosized zirconium phosphate (hereafter ZP) was used as starting material for the synthesis of ZP(AEP)$_x$ and it was prepared according to Pica et al. method.[33] The gel contained about 8 wt% of ZP.

ZP(AEP)$_x$ compounds have been prepared by topotactic anion exchange reaction of the phosphate groups of nanosized ZP with AEP groups. Specifically, a suitable volume of aqueous solutions of H_2AEP 0.3 M, 0.6 M or 0.8 M was added to 1 g of ZP in the form of gel in propanol (14 mL PrOH/1 g ZP), so that the H_2AEP/Zr molar ratio was 1, 2, 3, respectively, while the (PrOH/H_2O) volume ratio was 1 in all cases. The stirred mixture was then heated at 80°C for three days. The ZP(AEP)$_x$ samples were washed with a 10^{-3} M HCl solution in H_2O/PrOH (1:1 v/v) and then dried at 60°C for 15 hours. The samples were again washed with a 10^{-3} M HCl solution and finally dried at 60°C for 15 hours.

The AEP/Zr molar ratios (x) in ZP(AEP)$_x$ were determined by ICP and ^{31}P liquid NMR and the obtained values were reported in Table 1.

2. Preparation of gold nanoparticles supported on ZP(AEP)$_{0.72}$

ZP(AEP)$_{0.72}$ was selected as support for the synthesis and immobilization of AuNPs. In a typical experiment, 150 mg of ZP(AEP)$_{0.72}$ were suspended in 6.0 mL (or 15 mL) of water, then, 0.26 mL (or 0.62 mL) of a 0.03 M $HAuCl_4$ solution was added, so as to obtain materials with 1 and 2.4 wt% of Au loading. The mixtures were left under stirring at room temperature for about one day. Then, 0.39 mL (or 0.94 mL) of a 0.4 M freshly prepared $NaBH_4$ solution was added: the $NaBH_4$/Au(III) molar ratio was around 20 in both experiments. The solution color immediately turned from pale yellow to pink/plum. The experimental conditions used for the preparation of the catalysts are summarized in Table 6. The color of the mixture immediately turned from pale yellow to pink/plum. The solids were recovered by centrifugation, washed with water and dried at room temperature over P_2O_5.

Table 8. Experimental conditions for the synthesis and composition data of Au@ZP(AEP).

$HAuCl_4$ 0.03 M (mL)	$NaBH_4$ 0.4 M (mL)	$NaBH_4$/Au molar ratio	Au loading (wt%)[a]
0.26	0.39	20	1.0
0.62	0.94	20	2.4

[a] Calculated by ICP analysis. In the text the samples have been labelled as Au1@ZP(AEP) (Au loading = 1 wt%) and Au2.4@ZP(AEP) (Au loading = 2.4 wt%).

General procedure for catalytic reduction of nitroarenes

In a vial of 2 mL, Au1@ZP(AEP) catalyst (20 mg, 0.05 mmol of Au per g, 1 mol%), nitroarene (**1**, 0.1 mmol), $NaBH_4$ (22.8 mg, 6 eq) and EtOH$_{abs}$ or EtOH 96% (1.8 mL) were placed. The reaction mixture was stirred at 30 °C for a selected time (Table 2 and 3); the conversion of nitroarenes was monitored by GLC analyses. After completion, the solid catalyst was separated by centrifugation and then washed with EtOH (2 x 1 mL). The ethanol solution, that contained the products and the borate derived from $NaBH_4$, was distilled at reduced pressure, the residue was diluted with ethyl acetate (5 mL) and washed with water (2 x 2 mL). The organic layers were dried with sodium sulfate and evaporated under reduced pressure. The solid catalyst was washed with aqueous HCl 10^{-2} M to eliminate the borate, water and finally with EtOH, dried at 130 °C for 15 h and reused in the next cycle.

3,3'-di-(1-hydroxyethyl)azoxybenzene (2j). Purification by column chromatography on silica gel eluting with hexane/ethyl acetate (6:4). Obtained 11.4 mg of a pale yellow oil (80%).

^{1}HNMR (400 MHz) δ: 1.50 (s, 3H), 1.54 (s, 3H), 2.52 (s, 2H), 4.90-4.99 (m, 2H), 7.38-7.48 (m, 3H), 7.52-7.54 (d, 1H, J = 7.6 Hz), 8.04-8.06 (d, 1H, J = 7.8 Hz), 8.08 (s, 1H), 8.12-8.14 (d, 1H, J = 8 Hz), 8.25 (s, 1H).

^{13}CNMR (100.6 MHz) δ: 25.120, 25.26, 69.69, 70.03, 119.26, 121.18, 122.66, 124.27, 126.73, 128.63, 128.80, 128.92, 143.87, 146.48, 147.13, 148.24.

GC-MS (m/z): 286 (41), 242 (5), 195 (5), 181 (15), 169 (8), 149 (8), 121 (88), 103 (100), 93 (30), 91 (24), 77 (56), 65 (20), 51 (11).

Anal. Calcd for $C_{16}H_{18}N_2O_3$ (286.13): C, 67.12; H, 6.34; N, 9.78; Found C, 66.93; H, 6.42; N, 9.59.

Typical procedure for a sustainable protocol for the preparation of 4a

In a vial of 10 mL, Au1@ZP(AEP) catalyst (100 mg, 0.05 mmol of Au per g, 1 mol %), 4-nitroanisole **1a** (76.5 mg, 0.5 mmol), $NaBH_4$ (114 mg, 6 eq), and EtOH$_{abs}$ (9 mL) were placed. The reaction mixture was stirred at 30 °C for 2 h. After removal and recovery of the ethanol via distillation (90% of solvent recovered) the product was separated simple by washing the residue with cyclopenthyl methyl ether (3 x 2 mL). The solvent was evaporated by distillation (95% of solvent recovered) obtaining the pure product (yield of **4a** 96%). The solid catalyst was washed with aqueous HCl 10^{-2} M to eliminate the borate, water and finally with EtOH, dried at 130 °C for 15 h and reused in the next cycle.

E-factor calculation for product **4a** (yield 96%): E-factor = [0.0765 g (4-nitroanisole, **1a**) + 0.114 g ($NaBH_4$) + 0.100 g (Au1@ZP(AEP)) + 10.4 g (EtOH) – 0.059 g (4-methoxyaniline, **4a**)–0.095 g (recovered Au1@ZP(AEP)) – 9.5 g (recovered EtOH)/ 0.059 g (4-methoxyaniline, **4a**) = 17.6.

Without recover of reaction medium the E-factor value was 178.6.

Typical procedure for a sustainable protocol for the preparation of 4a under <u>flow conditions</u>

A premixed mixture of **1a** (1.53 g, 10 mmol), NaBH$_4$ (1.13 g, 3 eq) and EtOH$_{abs}$ (40 mL)) was charged into a glass column functioning as a reservoir. The equipment was connected, by using the appropriate valves, to a pump and installed into a box thermostated at 30 °C. The reaction mixture was continuously pumped (flow rate: 0.1 mL·min-1; residence time: 50 min) through the catalyst column (15 cm, stainless steel HPLC column) equipped with a 120 psi back pressure regulator, and the reaction was monitored by GC. Product was collected in fractions and gold content in the EtOH solution was periodically measured by ICP-OES analysis. After completion 20 mL of EtOH was used to wash the catalyst inside the reactor. After removal and recovery of the solvent via distillation (90% of solvent recovered) the product was separated simple by washing the residue with cyclopenthyl methyl ether (3 x 15 mL). The solvent was evaporated by distillation (95% of solvent recovered) obtaining the pure product (yield of **4a** 97%). The catalyst inside the column was dried under N$_2$ flow at 180 °C and reused in the next cycle.

E-factor calculation for product **4a** (yield 97%): E-factor = [1.5 g (4-nitroanisole, **1a**) + 1.13 g (NaBH$_4$) + 32 g (EtOH) + 39 g (CPME) – 1.2 g (4-methoxyaniline, **4a**) – 29 g (recovered EtOH)] – 37 g (recovered CPME)] / 1.2 g (4-methoxyaniline, **4a**) = 5.4

Typical procedure for a sustainable protocol for the preparation of 2a under <u>flow conditions</u>

A premixed mixture of **1a** (2,29 g, 15 mmol), NaBH$_4$ (1.7 g, 3 eq) and and EtOH 96 %. (60 mL)) was charged into a glass column functioning as a reservoir. The equipment was connected, by using the appropriate valves, to a pump and installed into a box thermostated at 30 °C. The reaction mixture was continuously pumped (flow rate: 0.1 mL·min-1; residence time: 50 min) through the catalyst column (15 cm, stainless steel HPLC column) equipped with a 120 psi back pressure regulator, and the reaction was monitored by GC. Product was collected in fractions and gold content in the EtOH solution was periodically measured by ICP-OES analysis. After completion 20 mL of EtOH was used to wash the catalyst inside the reactor. After removal and recovery of the solvent via distillation (90% of solvent recovered) the product was separated simple by washing the residue with cyclopenthyl methyl ether (3 x 18 mL). The solvent was evaporated by distillation (95% of solvent recovered) obtaining the pure product (yield of **2a** 90%). The catalyst inside the column was dried under N$_2$ flow at 180 °C and reused in the next cycle.

E-factor calculation for product **2a** (yield 90%): E-factor = [2.3 g (4-nitroanisole, **1a**) + 1.7 g (NaBH$_4$) + 47 g (EtOH) + 46 g (CPME) – 3.5 g (azoxyderivative, 2**a**) – 42 g (recovered EtOH)] – 44 g (recovered CPME)] / 3.5 g (4-methoxyaniline, **2a**) = 2.1

Conflicts of interest

There are no conflicts of interest to declare.

Acknowledgements

View Article Online
DOI: 10.1039/C8GC03513J

The Università degli Studi di Perugia and MIUR is acknowledged for financial support to the project AMIS, through the program "Dipartimenti di Eccellenza - 2018-2022". The authors would like to thank Prof. Paola Sassi for the FTIR analysis, Dr Fabio Marmottini for surface area measurements and Dr Alessandro di Michele for SEM analysis.

Notes and references

‡ Experimental Section and representative E-factor calculation, full characterization of compounds and copies of the ^{1}H and ^{13C} NMR spectra. This material is available free of charge via the Internet at http://pubs.acs.org.

1 (a) R. A. Sheldon *Green Chem*. 2017, **19**, 18-43; (b) R. A. Sheldon, I. Arends, U. Hanefeld, *Green Chemistry and Catalysis.* Wiley-VCH: Weinheim, 2007.
2 (a) S. Hübner, J. G. de Vries, V. Farina, *Adv. Synth. Catal.* 2016, **358**, 3–25; (b) D. Roy, Y. Uozumi, *Adv. Synth. Catal.* 2018, **360**, 602-625.
3 (a) B. Altava, M. I. Burguete, E. García-Verdugo, S. V. Luis, *Chem. Soc. Rev.* 2018, **47**, 2722-2771; (b) S. Santoro, S. I. Kozhushkov, L. Ackermann, L. Vaccaro, *Green Chem*. 2016, **18**, 3471-3493; (b) L. Liu, A. Corma, *Chem. Rev.* 2018, **118**, 4981–5079; (c) R. Van Santen in Modern Heterogeneous Catalysis. An Introduction. Weinheim: Wiley-VCH, 2017, (d) Rothenberg, G. (2017). Catalysis: Concepts and Green Applications. (2 ed.) Weinheim: Wiley-VCH, 2017.
4 For selected examples see: (a) S. Santoro, A. Marrocchi, D. Lanari, L. Ackermann, L. Vaccaro, *Chem. Eur. J.* 2018, **24**, 13383–13390; (b) F. Ferlin, V. Trombettoni, L. Luciani, S. Fusi, O. Piermatti, S. Santoro, L. Vaccaro, *Green Chem.* 2018, **20**, 1634–1639; (c) L. Luciani, E. Goff, D. Lanari, S. Santoro, L. Vaccaro, *Green Chem.* 2018, **20**, 183–187; (d) S. Santoro, F. Ferlin, L. Luciani, L. Ackermann, L. Vaccaro, *Green Chem.* 2017, **19**, 1601–1612; (e) F. Fringuelli, D. Lanari, F. Pizzo and L. Vaccaro, *Green Chem.*, 2010, **12**, 1301-1305; (f) S. Bonollo, F. Fringuelli, F. Pizzo and L. Vaccaro, *Synlett*, 2007, 2683–2686; (g) L. Castrica, F. Fringuelli, L. Gregoli, F. Pizzo and L. Vaccaro, *J. Org. Chem.*, 2006, **71**, 9536–9539; (h) F. Fringuelli, F. Pizzo and L. Vaccaro, *Synlett*, 2000, 311–314.
5 (a) E. Petricci, C. Risi, F. Ferlin, D. Lanari, L. Vaccaro, *Scientific Rep.* **2018**, *8*, 10571; (b) F. Ferlin, L. Luciani, S. Santoro, A. Marrocchi, D. Lanari, A. Bechtoldt, L. Ackermann, L. Vaccaro. *Green Chem.* 2018, **20**, 2888–2893; (c) F. Ferlin, S. Santoro, L. Ackermann and L. Vaccaro, *Green Chem.*, 2017, **19**, 2510–2514; (b) D. Rasina, A. Kahler-Quesada, S. Ziarelli, S. Warratz, H. Cao, S. Santoro, L. Ackermann and L. Vaccaro, *Green Chem.*, 2016, **18**, 5025–5030; (c) X. Tian, F. Yang, D. Rasina, M. Bauer, S. Warratz, F. Ferlin, L. Vaccaro and L. Ackermann, *Chem. Commun.*, 2016, **52**, 9777–9780; (d) G. Strappaveccia, E. Ismalaj, C. Petrucci, D. Lanari, A. Marrocchi, M. Drees, A. Facchetti and L. Vaccaro, *Green Chem.*, 2015, **17**, 365–372; (e) G. Strappaveccia, L. Luciani, E. Bartollini, A. Marrocchi, F. Pizzo and L. Vaccaro, *Green Chem.*, 2015, **17**, 1071–1076; (f) E. Ismalaj, G. Strappaveccia, E. Ballerini, F. Elisei, O. Piermatti, D. Gelman and L. Vaccaro, *ACS Sustainable Chem. Eng.*, 2014, **2**, 2461–2464.
6 (a) B. C. Gates, *Chem. Rev.* 1995, **95**, 511-522; (b) *Nanomaterials in Catalysis*, P. Serp, K. Philippot, Eds.; Wiley-VCH, RSC Catalysis series, 2013, No. **17**; (c) *Metal Nanoparticles for catalysis: Advances and Application*, F. Tao, Ed.; 2014, Royal Society of Chemistry.

View Article Online
DOI: 10.1039/C8GC03515J

7 In Heterogeneous Gold Catalysts and Catalysis, Z. Ma, S. Dai, Eds; RSC Catalysis series 2014, No. **18**, Ch.1, Royal Society of Chemistry.

8 (a) *Nanoparticles and Catalysis*, D. Astruc, Ed.; Wiley-VCH 2008, Weinheim; (b) J. M. Campelo, D. Luna, R. Luque, J. M. Marinas, A. A. Romero, *ChemSusChem* 2009, **2**, 18-45; (c) C. Lin, K. Tao, D. Hua, Z. Ma, S. Zhou, *Molecules* 2013, **18**, 12609-12620; (d) K. Shimizu, Y. Miyamoto, T. Kawasaki, T. Tanji, Y. Tai, A. Satsuma, *J. Phys. Chem. C,* 2009, **113**, 17803–17810.

9 (a) S. A. Lawrence, *Amines: Synthesis, Properties and Applications*, Cambridge University Press: New York, 2004; (b) S. Nishimura, *Handbook of Heterogeneous Catalytic Hydrogenation for Organic Synthesis*, Wiley, Chichester, 2001, pp. 315–387; (c) D. H. Rosenblatt, E. P. Burrows, *The Chemistry of Amino Nitroso and Nitro Compounds and their Derivatives*, Wiley-VCH, Chichester, 1982, pp. 1085; (d) S. C. Mitchell, R. H. Waring In *Ullmanns Encyclopedia of Industrial Chemistry*, Wiley-VCH, Weinheim, Germany, 2000.

10 (a) H.-U. Blaser; H. Steiner, M. Studer, *ChemCatChem* 2009, **1**, 210-221; (b) H. K. Kadama, S. G. Tilve, *RSC Adv.* 2015, **5**, 83391-83407; (c) R. Begum, R. Rehan, Z. H. Farooqi, Z. Butt, S. Ashraf, *J. Nanopart. Res.* 2016, **18**, 231; (d) R. Sedghi, M. M. Heravi, S. Asadi, N. Nazari, M. R. Nabid, *Current Organic Chemistry* 2016, **20**, 696-734.

11 (a) N. Sakai, K. Fujii, S. Nabeshima, R. Ikeda, T. Konakahara, *Chem. Commun.* 2010, **46**, 3173-3175; (b) J. H. Kim, J. H. Park, Y. K. Chung, K. H. Park, *Adv. Synth. Catal.* 2012, **354**, 2412-2418; (c) X. Liu, S. Ye, H.-Q. Li, Y.-M. Liu, Y. Cao, K.-N. Fan, *Catal. Sci. Technol.* 2013, **3**, 3200-3206.

12 (a) S. Fountoulaki, V. Daikopoulou, P. L. Gkizis, I. Tamiolakis, G. S. Armatas, I. N. Lykakis, *ACS Catal.* 2014, **4**, 3504-3511; (b) A. Noschese, A. Buonerba, P. Canton, S. Milione, C. Capacchione, A. Grassi, *J. Catal.* 2016, **340**, 30-40; (c) P. Fakhri, M. Nasrollahzadeh, B. Jaleha, *RSC Adv.* 2014, **4**, 48691-48697; (d) L. C. Moraes, B. Lacroix, R. C. Figueiredo, P. Lara, J. Rojo, S. Conejero, *Dalton Trans.* 2017, **46**, 8367-8371; (e) C. Wang, W. Zou, J. Wang, Y. Ge, R. Lu, S. Zhang, *New J. Chem.* 2017, **41**, 3865-3871; (f) K. Lamei, H. Eshghi, M. Bakavoli, S. Rostamnia, *Catal. Lett.* 2017, **147**, 491-501; (g) Y. Su, X. Li, Y. Wang, H. Zhong, R. Wang, *Dalton Trans.* 2016, **45**, 16896-16903.

13 (a) S. Park, I. S. Lee, J. A. Park, *Org. Biomol. Chem.* 2013, **11**, 395-399.

14 (a) X.-B. Lou, L. He, Y. Qian, Y.-M. Liu, Y. Cao, K.-N. Fan, *Adv. Synth. Catal*. 2011, **353**, 281-286; (b) Q. Zhang, S.-S. Li, M.-M. Zhu, Y.-M. Liu, H.-Y. He, Y. Cao, *Green Chem.* 2016, **18**, 2507-2513; (c) L. Yu, Q. Zhang, S.-S. Li, J. Huang, Y.-M. Liu, H.-Y. He, Y. Cao, *ChemSusChem* 2015, **8**, 3029-3035.

15 H. Zhu, X. Ke, X. Yang, S. Sarina, H. Liu, *Angew. Chem. Int. Ed.* 2010, **49**, 9657-9661.

16 Z. Yan, Q. Chen, P. Xia, W. Ma, B. Ren, *Nanotechnology* 2016, **27**, 035707/1-11.

17 veg(a) Wang, X.; Li, M.; Keane M. A. *In Heterogeneous Gold Catalysts and Catalysis*, Ma, Z.; Dai S., Eds; RSC Catalysis series 2014, No. 18, Ch 11, Royal Society of Chemistry; (b) Corma, A.; Garcia, H. Supported Gold Nanoparticles as Catalysts for Organic Reactions **.** *Chem. Soc. Rev.* 2008, **37**, 2096-2126.

18 (a) S. L. Westcott, S. J. Oldenburg, T. RLee, N. J. Halas, *Langmuir* 1998**, 14***,* 5396-5401; (b) M. Aslam, L. Fu, M. Su, K. Vijayamohanan, V. P. Dravid, *J. Mater. Chem.* 2004, **14**, 1795–1797; (c) T. Sainsbury, T. Ikuno, D. Okawa, D. Pacilé, J. M. J. Fréchet, A. Zettl, *J. Phys. Chem. C* 2007, **111***,* 12992-12999.

19 (a) C. Petrucci, M. Cappelletti, O. Piermatti, M. Nocchetti, M. Pica, F. Pizzo, L. Vaccaro, *J. Mol. Catal. A Chem.* 2015, **401**, 27–34; (b) F. Costantino, R. Vivani, M. Bastianini, L. Ortolani, O. Piermatti, M. Nocchetti, L. Vaccaro, *Chem. Commun.* 2015, **51**, 15990–15993; c) V. Kozell, T. Giannoni, M. Nocchetti, R. Vivani, O. Piermatti, L. Vaccaro, *Catalysts* 2017, **7**, 186–206.

20 (a) U. Costantino, F. Fringuelli, M. Nocchetti, O. Piermatti, *App. Catal. A: General* 2007, **326**, 100-105; (b) U. Costantino, F. Fringuelli, M. Orrù, M. Nocchetti, O. Piermatti, F. Pizzo, *J. Org. Chem.* 2009, 1214-1220; (c) A. Cipiciani, U. Costantino, F. Bellezza, F. Fringuelli, M. Orrù, O. Piermatti, F. Pizzo, *Catal. Today* 2010, **152**, 61-65; (d) D. Lanari, F. Montanari, F. Marmottini, O. Piermatti, M. Orrù, L. Vaccaro, . *J. Catal.* 2011, **277**, 80-87; (e) S. Calogero, D. Lanari, M. Orrù, O. Piermatti, F. Pizzo, L. Vaccaro, *J. Catal.* 2011, **282**, 112-119; (f) M. Angeloni, O. Piermatti, F. Pizzo, L. Vaccaro, *Eur. J. Org. Chem.* 2014, 1716–1726.

21 (a) A. Clearfield, U. Costantino, In *Comprehensive Supramolecular Chemistry*, G. Alberti, T. Bein, Eds; Elsevier Science Ltd. Press: New York, 1996; Vol. **7**, Ch. 4 and 5.

22 (a) M. Pica, A. Donnadio, E. Troni, D. Capitani, M. Casciola, *Inorg. Chem.* 2013, **52**, 7680-7687; b) M. Pica, A. Donnadio, R. D'Amato, D. Capitani, M. Taddei, M. Casciola, *Inorg. Chem.* 2014, **53**, 2222-2229.

23 (a) M. Casciola, U. Costantino, A. Peraio, T. Rega, *Solid State Ionics* 1995, **77**, 229-233.

24 (a) G. Kortuem in *Reflectance Spectroscopy*, Springer-Verlag, Berlin, Heidelberg: New York, 1969.

25 T. Nakamura, Y. Yamada, K. Yano, *J. Mater. Chem.* 2007, **17**, 3726–3732.

26 Link, S.; El-Sayed, M. A. Size and Temperature Dependence of the Plasmon Absorption of Colloidal Gold Nanoparticles. *J. Phys. Chem. B*, 1999, **103**, 4212-4217.

27 (a) S-. E. Horsley, D. V. Nowell, D. T. Stewart, Spectrochim. Acta A 1974, **30**, 535–541; (b) M. Taddei, P. Sassi, F. Costantino, R. Vivani, *Inorg. Chem.* 2016**, 55**, 6278–6285.

28 (a) S. Ghosh, A. N. Harke, M. J. Chacko, S. P. Gurav, K. A. Joshi, A. Dhepe, A. Dewle, G. B. Tomar, R. Kitture, V. S. Parihar, K. BanerjeeN. Kamble, J. Bellare, B. A. Chopade, *J Nanomed. Nanotechnol* 2016, ***7***, 1000390; (b) M. Casciola, A. Donnadio, M. Pica, V. Valentini, P. Piaggio, *Macromol. Symp.,* 2005, **230**, 95–104.

29 W.-G. Jia, H. Zhang, T. Zhang, D. Xie, S. Ling, E.-H. Sheng, *Organometallics* 2016, **35**, 503-512.

30 C. Z. Zhang, H. Yang, D.-L. Wu, G.-Y. Lu, *Cinese J. Chem.* 2007, **25**, 653-660.

31 (a) Y. Liu, B. Liu, A. Guo, Z. Dong, S. Jin, Y. Lu, *Synth. Commun.* 2012, **42**, 2201-2206.

32 (a) Y. Liu, B. Liu, A. Guo, Z. Dong, S. Jin, Y. Lu, *Molecules* 2011, **16**, 3563-3568.

33 M. Pica, A. Donnadio, D. Capitani, R. Vivani, R. Troni, E.; M. Casciola, *Inorg. Chem.* 2011, ***50***, 11623–11630.